

Effects of Crystallization Temperature of Poly(vinylidene fluoride) on Crystal Modification and Phase Transition of Poly(butylene adipate) in Their Blends: A Novel Approach for Polymorphic Control

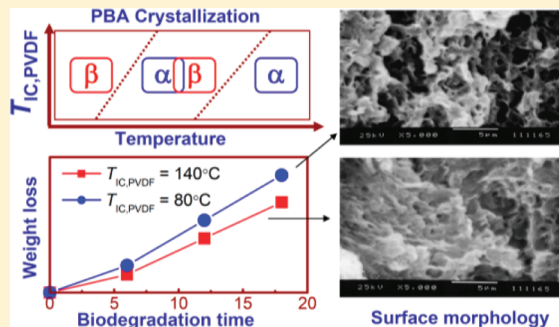
Jinjun Yang,^{*,†,‡} Pengju Pan,^{*,‡,§} Lei Hua,[‡] Xin Feng,[†] Junjie Yue,[†] Yanhui Ge,[†] and Yoshio Inoue[‡]

[†]School of Environmental Science and Safety Engineering, Tianjin University of Technology, Tianjin 300384, China

[‡]Department of Biomolecular Engineering, Tokyo Institute of Technology, 4259-B-55 Nagatsuta, Midori-ku, Yokohama 226-8501, Japan

[§]State Key Laboratory of Chemical Engineering, Department of Chemical and Biological Engineering, Zhejiang University, 38 Zheda Road, Hangzhou 310027, China

ABSTRACT: Effects of the isothermal crystallization temperatures of poly(vinylidene fluoride), $T_{IC,PVDF}$, on polymorphic crystalline structure, phase transition, fractional crystallization, and enzymatic degradation of poly(butylene adipate) (PBA) in crystalline/crystalline blends have been investigated. The crystal modifications of PBA can be regulated by $T_{IC,PVDF}$. Lower $T_{IC,PVDF}$ (e.g., 80 °C) facilitates the formation of PBA α crystals in both the isothermal and nonisothermal melt crystallizations and also favors the β -to- α phase transition of PBA upon annealing at elevated temperatures. This might be attributable to the decreased equilibrium melting temperature of PBA when $T_{IC,PVDF}$ is decreased. Higher $T_{IC,PVDF}$ is favorable for the fractional crystallization of PBA, which tends to segregate in the interlamellar regions of the PVDF matrix under these conditions. PBA shows faster enzymatic degradation in the blends with a lower $T_{IC,PVDF}$ than those with a higher $T_{IC,PVDF}$, attributable to the preferential formation of α crystals at a lower $T_{IC,PVDF}$. This study provides a new method to control the crystal modification and physical properties of polymorphic polymers in their blend systems.



1. INTRODUCTION

Polymorphism in polymer science represents the existence of more than one crystal form or crystalline structure in a solid state with the same chemical composition. It describes different crystal packing arrangements of the same molecular species in its crystalline unit cells.¹ Polymorphism has been found in many semicrystalline polymers such as syndiotactic polypropylene (s-PP),² isotactic polypropylene (i-PP),^{3,4} poly(L-lactide) (PLLA),⁵ poly(3-hydroxypropionate) (PHP),⁶ and poly(butylene adipate) (PBA).^{7–9} Almost all of the semicrystalline polymers can show polymorphism with changing crystallization conditions. Because the crystalline forms usually have distinct physical properties (e.g., mechanical, electrical, and biodegradable properties), regulating the crystal modification of polymorphic polymers is an efficient method to tailor their physical performances. In addition to the crystallization temperature, crystallization methods (e.g., melt, cold, or solution crystallization), and stress treatment (or orientation), the crystal modifications of polymorphic polymers can be manipulated by other factors such as the molecular weight, microstructure of the polymer chain,² fusion temperature prior to crystallization,^{10,11} epitaxial crystallization,^{12–15} and nucleating agent.^{16–19}

Polymer blending is a simple, economical, and most widely used approach to produce new polymeric materials with desired

properties. Among the blend systems, the miscible crystalline/crystalline blends are of great interest because they exhibit a wide variety of morphologies depending on the thermal conditions.^{20,21} For the binary crystalline/crystalline blends where the blend components have distinct melting point (T_m) and crystallization temperature (T_c), two-step crystallization occurs. During the cooling or two-step isothermal melt-crystallization (IC), the high- T_m component crystallizes first, and the growth of crystal lamellae and spherulite would induce the positional phase segregation of the low- T_m component with respect to the crystalline phase of the high- T_m component, such as the interlamellar, interfibrillar, or interspherulitic segregation.^{22–24} The phase segregation of the low- T_m component in the crystallization of the high- T_m component would inevitably influence its crystallization kinetics and morphology, accompanying the fractional crystallization of the low- T_m component.^{22,23}

The miscible blending with amorphous polymer has been an effective method to control the crystal modification of polymorphic polymers due to the dilution effects of the amorphous component.^{10,25–28} Because blending is the most

Received: October 6, 2011

Revised: December 15, 2011

Published: January 7, 2012

common way to modify the properties of polymeric materials, the crystalline structural studies of polymorphic polymers in their blend systems are of fundamental importance. However, the polymorphic crystalline structures of the blend component in the crystalline/crystalline blends have been unexplored, except for our preliminary reports on the blend composition effects on crystallization kinetics and crystalline structure.²⁹ Previous study has reported that, besides the blend composition, T_c of the high- T_m component remarkably influences the phase segregation, distribution, and crystallization kinetics of the low- T_m component in their miscible crystalline/crystalline blends.^{22,23} For the poly(butylene succinate)/poly(ethylene oxide) (PBS/PEO) blends, the higher T_c of the high- T_m component, PBS, induces the segregation of the PEO phase in the interlamellar region of PBS crystals, resulting in the crystallization of partial PEO at a significant large supercooling.^{22,23} However, is it possible to control the crystal modification and physical properties of low- T_m component via changing the crystallization conditions (especially the T_c) of the high- T_m component? Herein, we would like to present a study of regulating the crystalline structure and physical properties of a semicrystalline polymer via changing the crystallization condition of its blend pair.

Poly(vinylidene fluoride) (PVDF) and PBA are both crystalline polymers, with a T_m gap of about 110 °C and good miscibility over the entire composition range.^{30–35} PVDF has a $T_{m,PVDF}$ of ~165 °C and a $T_{c,PVDF}$ of ~140 °C. The $T_{m,PBA}$ and $T_{c,PBA}$ of PBA are ~55 and ~30 °C, respectively. Depending on the thermal conditions, PVDF/PBA blends can exist in a single-phase amorphous state ($T > T_{m,PVDF}$), a crystalline/amorphous state ($T_{m,PBA} < T < T_{m,PVDF}$), or a crystalline/crystalline state ($T < T_{m,PBA}$). PBA is a biodegradable polyester that can form polymorphic crystalline structures (α and β forms) with changing crystallization temperature.^{7–9} The α and β crystals of PBA are produced in the melt crystallization at temperatures above 32 °C and below 28 °C, respectively.^{7–9} The β crystals transform into their α counterparts upon heating or annealing at a high temperature.⁸ The α - and β -form PBAs have distinct enzymatic degradation rates. The PBA α crystals, which are thermodynamically stable, have the faster biodegradation than their β counterparts.³⁶ Because of the distinct enzymatic degradation rate and thermal stability between the crystalline forms, manipulating the crystal modifications of PBA would be an ideal approach to tune its physical properties.^{11,14,15,18,19,37} Moreover, PVDF/PBA blends have unique morphological characteristics. PBA can segregate and crystallize within the PVDF interlamellar region,³⁴ affording diversified crystalline morphologies to this blend pair. Therefore, in this work, the PVDF/PBA blend was chosen as a model to regulate the crystal modification and physical properties of polymorphic polymers in the crystalline/crystalline blend systems. This blend system is considered to be an ideal example to investigate the correlations between the polymorphic crystalline structure, phase transition, fractional crystallization kinetics, and physical properties (e.g., biodegradation) of a blend component in the miscible crystalline/crystalline blend systems.

In a previous study, we have found that the crystallization kinetics and crystal modification of PBA are influenced by blending with PVDF, where only an effect of fixed crystallization condition (i.e., nonisothermal melt crystallization) of PVDF was studied.²⁹ In this work, we investigated the effects of the IC temperature of PVDF ($T_{IC,PVDF}$) on the crystal

modification, phase transition, fractional crystallization, and biodegradability of PBA in its blends. To the best of our knowledge, this represents the first report that the crystal modification, phase transition, and physical property of a semicrystalline polymer can be successfully regulated by changing the crystallization conditions of the other component in their miscible blends.

2. EXPERIMENTAL SECTION

2.1. Materials. PBA ($M_w = 12\,000$ Da) and PVDF ($M_w = 180\,000$ Da) were purchased from Aldrich Co. Before use, PBA was purified by precipitating into ethanol from the chloroform solution and then was dried under vacuum at 40 °C for 1 week. PVDF/PBA blends with different compositions were prepared by solution casting using DMF as a common solvent. The solutions of PBA and PVDF, both with the initial concentrations of 2 g/100 mL, were mixed with different volume proportions. These mixed solutions were cast on the polytetrafluoroethylene dishes. After the evaporation of solvent at 80 °C for 1 day, the resultant films were further dried under vacuum at 40 °C for 1 week. PVDF/PBA blends were marked as 10/90, 25/75, 50/50, 75/25, and 90/10, where the numerals denoted weight percentages of PVDF (C_{PVDF}) and PBA (C_{PBA}), respectively.

2.2. Differential Scanning Calorimetry (DSC) Analysis. Thermal behavior of PVDF/PBA blends was measured by a Pyris Diamond DSC instrument (Perkin-Elmer Inc., Waltham, U.S.A.) equipped with a Perkin-Elmer intracooler 2P cooling accessory. The temperature and heat flow were calibrated using an indium standard under nitrogen purging. Thermal procedures for the nonisothermal crystallization (NIC) of PBA in the blends are shown in Figure 1a. The blends were first

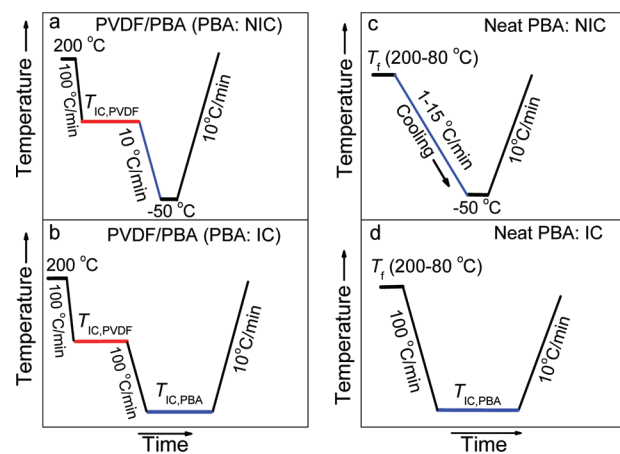


Figure 1. Thermal programs for nonisothermal (a,c) and isothermal (b,d) melt-crystallizations of the PBA component in PVDF/PBA blends (a,b) and neat PBA (c,d). The PVDF component was first isothermally melt-crystallized at $T_{IC,PVDF}$ in the blends.

heated to 200 °C and held at this temperature for 2 min to remove the thermal history. Then, the samples were quenched at a cooling rate of 100 °C/min to the predetermined $T_{IC,PVDF}$ (80–140 °C), which was much higher than $T_{m,PBA}$. After the complete crystallization of PVDF, the blends were cooled to –50 °C at a cooling rate of 10 °C/min for the nonisothermal melt crystallization of PBA. Finally, the samples were reheated to 200 °C at 10 °C/min to examine the melting behavior. Thermal procedures of nonisothermal crystallization and

subsequent melting of neat PBA are shown in Figure 1c, where T_f is the maximum fusion temperature. Thermal programs for the IC and subsequent melting of PBA in PVDF/PBA blends as well as neat PBA are presented in Figure 1b and d, respectively. In these experiments, the blends were quickly cooled to the crystallization temperature of PBA ($T_{IC,PBA}$) for melt crystallization after the isothermal crystallization of PVDF at $T_{IC,PVDF}$.

2.3. Wide-Angle X-ray Diffraction (WAXD) and Small-Angle X-ray Scattering (SAXS) Analyses. Thermal procedures of the samples for WAXD and SAXS measurements are the same to those used in DSC, as shown in Figure 1. The film samples for WAXD and SAXS measurements were prepared by hot-pressing at 200 °C. For the nonisothermal crystallization of the PBA component in the blends (Figure 1a), the hot-pressed films were quickly transferred into an oven preset to $T_{IC,PVDF}$. After the crystallization of the PVDF component, the film samples were rapidly transferred to a Linkam-600 hot stage (Linkam Scientific Instrument Ltd., Surrey, U.K.) equipped with a liquid nitrogen cooling unit, in which the samples were cooled to -50 °C at a cooling rate of 10 °C/min. Finally, the samples were reheated to room temperature at a heating rate of 10 °C/min. For the isothermal crystallization of the PBA component in the blends (Figure 1b), the samples were directly thrown into a water bath preset to $T_{IC,PBA}$ after the isothermal crystallization of the PVDF component at $T_{IC,PVDF}$. For the annealing experiments of the PBA component, the blend samples were thrown into a water bath preset to 18 °C to obtain the pure β -form PBA after the isothermal crystallization of the PVDF component at $T_{IC,PVDF}$ and then were transferred into an oven and annealed at 48 °C for different periods (10, 30, and 60 min).

After the completion of crystallization or annealing, the blend samples were analyzed by WAXD and SAXS. WAXD and SAXS measurements were performed on a Rigaku RU-200 with Ni-filtered CuK α radiation ($\lambda = 0.1542$ nm), worked at 40 KV and 200 mA (Rigaku Corp., Tokyo, Japan). WAXD patterns were collected between Bragg angles of 5 and 50° at a scanning rate of 1°·min⁻¹. SAXS profiles of neat PVDF, PBA, and their blends with different thermal treatments were recorded in the 2 θ range of 0.1–2°. 2 θ was increased by 0.02°, and the scattering patterns were collected for 20 s in each step.

2.4. Fourier Transform Infrared (FTIR) Spectroscopy Analysis. FTIR measurements were carried out on an AIM-8800 automatic infrared microscope using the transmission mode (Shimadzu, Kyoto, Japan). The samples were sandwiched between two BaF₂ slides, and their thermal programs were the same as those used in DSC and WAXD measurements (Figure 1a and b). IR spectra were scanned and collected at 20 °C, with an accumulation of 32 scans and a resolution of 2 cm⁻¹.

2.5. Enzymatic Degradation. In the experiments of enzymatic degradation, the PVDF/PBA blend films, prepared by the same method as WAXD samples, were thermally treated by the sequential ICs of the PVDF component at $T_{IC,PVDF} = 80$ or 140 °C and the PBA component at $T_{IC,PBA} = 28$ °C. The film samples were cut into a square film with a dimension of 1 × 1 × 0.1 cm³. Each film was weighted and put into a small glass bottle with 1 mL phosphate buffer (0.1 M, pH = 7.4) containing 1 mg/mL lipase from *Pseudomonas* sp. (Sigma Co., St. Louis, U.S.A.). The bottles were placed on a mechanical shaker with a speed of 100 rpm and a temperature of 37 °C. The degradation times were set to 6, 12, and 18 h, respectively. The sample was transferred into a new bottle containing the

fresh lipase solution with the same volume and concentration after each 6 h. It was washed twice with distilled water and dried under vacuum for a week after degradation. The dried sample was weighted to calculate the weight loss, which was calculated by averaging the results of three independent measurements. The surface morphology of the degraded sample was examined by a JEOL JSM-5200 scanning electron microscopy (SEM) (Tokyo, Japan).

3. RESULTS AND DISCUSSION

3.1. Isothermal Crystallization of PBA in Blends.

Parts a and b of Figure 2 show the WAXD patterns of neat PBA melt-

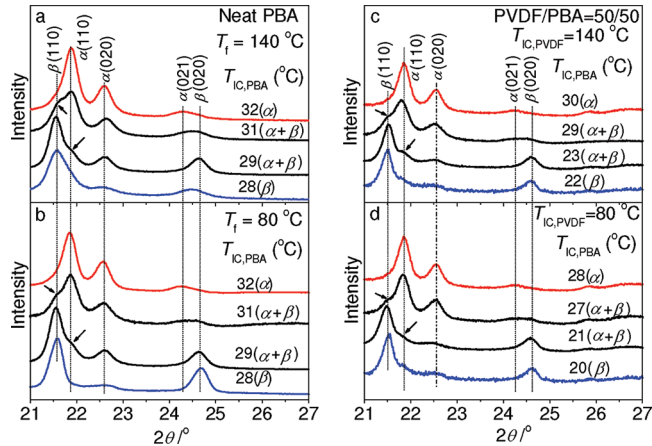


Figure 2. WAXD patterns of neat PBA melt-crystallized at different $T_{IC,PBA}$'s after quenching from $T_f = 140$ (a) and 80 °C (b). WAXD patterns of PVDF/PBA blends with $C_{PVDF} = 50\%$ after the sequential isothermal crystallizations of PVDF at $T_{IC,PVDF} = 140$ (c) or 80 °C (d) and PBA at different $T_{IC,PBA}$'s.

crystallized at different $T_{IC,PBA}$'s after being quenched from $T_f = 140$ and 80 °C, respectively. As seen in the figure, the $T_{IC,PBA}$ -dependent crystalline structure of neat PBA is not affected by T_f when T_f is much higher than $T_{m,PBA}$. Neat PBAs melt-crystallized at $T_{IC,PBA} \geq 32$, ≤ 28 , and 29–31 °C show the characteristic WAXD peaks of the α , β , and α/β mixed crystals, respectively. However, after blending with PVDF, the crystalline structure of PBA is influenced by $T_{IC,PVDF}$, which is equal to the T_f of the PBA component. Figure 2c and d shows WAXD patterns of the blends after the sequential isothermal crystallizations of PVDF at $T_{IC,PVDF} = 140$ or 80 °C and PBA at different $T_{IC,PBA}$'s. For the blend with $C_{PVDF} = 50\%$, the critical crystallization temperature regions for the formation of pure α and β crystals of PBA are $T_{IC,PBA} \geq 30$ and ≤ 22 °C at $T_{IC,PVDF} = 140$ °C (Figure 2c), while they are, respectively, decreased to $T_{IC,PBA} \geq 28$ and ≤ 20 °C at $T_{IC,PVDF} = 80$ °C. Similar trends are observed in the blends with other compositions (data not shown).

The FTIR spectrum of PBA is sensitive to its crystal modification because of the difference in the packing manner and conformation of polymer chains within the crystal unit cells.^{38,39} The β -form PBA has a characteristic band at 930 cm⁻¹.^{38,39} Figure 3 shows the FTIR spectra in the wavenumber region of 1000–900 cm⁻¹ for the PVDF/PBA blend ($C_{PVDF} = 50\%$) after the sequential crystallizations of PVDF at $T_{IC,PVDF} = 140$ or 80 °C and PBA at different $T_{IC,PBA}$'s. The corresponding second derivatives of these spectra are included to clearly identify the weak peaks. The IR bands shown in Figure 3 are

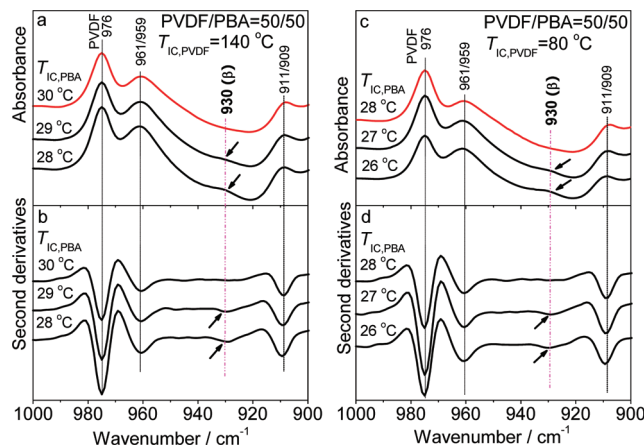


Figure 3. FTIR spectra and their corresponding second derivatives in the wavenumber region of 1000–900 cm⁻¹ for the PVDF/PBA blend ($C_{\text{PVDF}} = 50\%$) after the sequential isothermal crystallizations of PVDF at $T_{\text{IC},\text{PVDF}} = 140$ (a,b) or 80 °C (b,c) and PBA at different $T_{\text{IC},\text{PBA}}$'s.

assigned to the PBA component, except for the band at 976 cm⁻¹. When the $T_{\text{IC},\text{PVDF}}$ is 140 °C, the characteristic band of PBA β crystals at 930 cm⁻¹ appears at $T_{\text{IC},\text{PBA}} \leq 29$ °C but disappears at $T_{\text{IC},\text{PBA}} \geq 30$ °C (Figure 3a), indicative of the exclusive formation of α crystals at $T_{\text{IC},\text{PBA}} \geq 30$ °C. When the $T_{\text{IC},\text{PVDF}}$ is 80 °C, the critical formation temperature for the pure α crystals of PBA decreases to 28 °C in the blend with $C_{\text{PVDF}} = 50\%$ (Figure 3c). Both the WAXD and FTIR results suggest that the lower $T_{\text{IC},\text{PVDF}}$ facilitates formation of α -form PBA in the blends. The critical (or minimum) temperature for the formation of α -form PBA, denoted as $T_{\text{c},\alpha,\text{PBA}}$, is plotted as a function of C_{PVDF} in Figure 4. It can be seen that $T_{\text{c},\alpha,\text{PBA}}$'s of

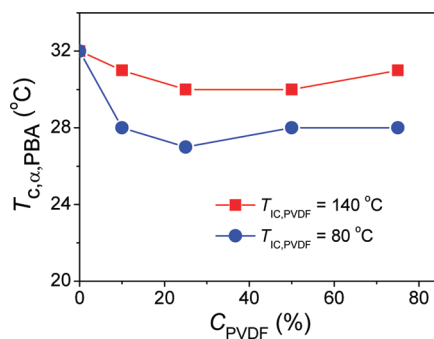


Figure 4. $T_{\text{c},\alpha,\text{PBA}}$ of PBA in PVDF/PBA blends with various compositions.

the blends with PVDF crystallized at a higher $T_{\text{IC},\text{PVDF}}$ (140 °C) are 2–3 °C higher than those with PVDF crystallized at a lower $T_{\text{IC},\text{PVDF}}$ (80 °C).

In order to calculate T_m^0 of the PBA α crystals, we investigated the melting behavior of PBA in the blends. Figure 5 shows the DSC heating curves of PBA in the blends after the sequential crystallizations of PVDF at $T_{\text{IC},\text{PVDF}} = 140$ or 80 °C and PBA at different $T_{\text{IC},\text{PBA}}$'s. DSC curves with the PBA component crystallized at $T_{\text{IC},\text{PBA}} \geq 30$ °C are only shown here. The double melting peaks of α -form PBA shown in Figure 5 are ascribed to the melt-recrystallization mechanism.^{8,9} The melting peak at lower temperature was used to calculate T_m^0 of PBA α crystals via the Hoffman–Weeks method.⁴⁰ The T_m^0 values of PBA component in the blends are listed in Table 1. As

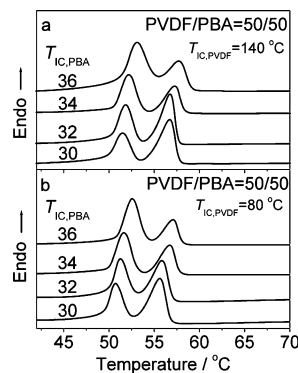


Figure 5. DSC heating curves of PBA in the PVDF/PBA blend ($C_{\text{PVDF}} = 50\%$) after the sequential isothermal crystallizations of PVDF at $T_{\text{IC},\text{PVDF}} = 140$ (a) or 80 °C (b) and PBA at different $T_{\text{IC},\text{PBA}}$'s.

Table 1. Thermal Parameters in Nonisothermal Melt Crystallization and Subsequent Melting of PBA in PVDF/PBA Blends with PVDF Crystallized at Different $T_{\text{IC},\text{PVDF}}$'s

sample	T_m^0 of PBA		nonisothermal crystallization of PBA					
	$T_{\text{IC},\text{PVDF}} = 140$ °C	$T_{\text{IC},\text{PVDF}} = 80$ °C	$T_{\text{IC},\text{PVDF}} = 140$ °C	$T_{\text{IC},\text{PVDF}} = 80$ °C	ΔH_c (J/g)	ΔH_m (J/g)	ΔH_c (J/g)	ΔH_m (J/g)
PVDF/PBA = 0/100	61.3	61.5	−60.6	61.5	−60.8	61.7		
PVDF/PBA = 10/90	59.1	57.3	−52.5	59.4	−58.3	57.1		
PVDF/PBA = 25/75	56.5	54.8	−50.7	53.8	−54.2	49.8		
PVDF/PBA = 50/50	57.5	55.6	−44.3	48.6	−49.2	44.9		
PVDF/PBA = 75/25	57.6	55.7	−25.8	26.1	−31.7	22.8		
PVDF/PBA = 90/10	UD ^a	UD	UD	UD	UD	UD	UD	UD

^aUnable to determine.

seen in this table, T_m^0 of PBA in the blends with PVDF crystallized at $T_{\text{IC},\text{PVDF}} = 80$ °C is about 2 °C lower than those with $T_{\text{IC},\text{PVDF}} = 140$ °C. As $T_{\text{IC},\text{PVDF}}$ is decreased, the decrease of T_m^0 can shift the crystallization of the PBA component to the lower temperature range, leading to a favorable formation of α -form PBA.

3.2. Nonisothermal Crystallization of PBA in Blends.

The crystalline structure of the PBA component non-isothermally crystallized in the blends was investigated via WAXD analysis. Figure 6a shows the WAXD patterns of neat PBA nonisothermally crystallized at different cooling rates. The crystal modification of neat PBA changes from the α to β form as the cooling rate is increased from 2.5 to 15 °C/min because the small cooling rate induces the crystallization of PBA at high temperature (Figure 6a). Figure 6b–d shows WAXD patterns of the blends ($C_{\text{PVDF}} = 25$, 50, and 75 wt %) after the crystallization of PVDF at $T_{\text{IC},\text{PVDF}} = 140$ or 80 °C and the nonisothermal crystallization of PBA at a cooling rate of 10 °C/min. As seen in these figures, the α/β mixed crystals of PBA are developed at $T_{\text{IC},\text{PVDF}} = 140$ °C, while the α crystals are exclusively produced at $T_{\text{IC},\text{PVDF}} = 80$ °C in the blends with different compositions. The lower $T_{\text{IC},\text{PVDF}}$ is favorable to produce the α crystals during the nonisothermal crystallization of the PBA component.

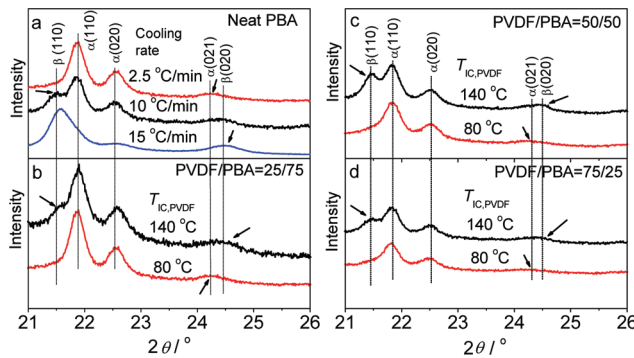


Figure 6. WAXD patterns of neat PBA nonisothermally melt-crystallized at different cooling rates (a). WAXD patterns of the blends with C_{PVDF} = 25 (b), 50 (c), and 75% (d) after the isothermal crystallization of PVDF at T_{IC,PVDF} = 140 or 80 °C and the nonisothermal crystallization of PBA at a cooling rate of 10 °C/min.

The nonisothermal crystallization of the PBA component in its blends was further investigated via DSC. Figure 7 shows the

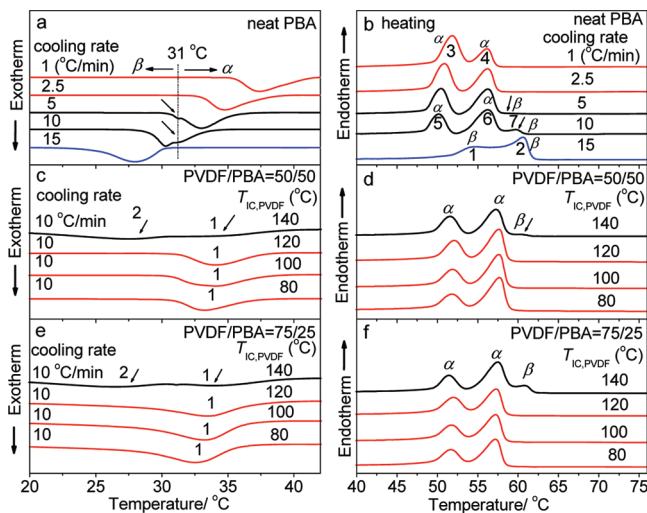


Figure 7. DSC curves recorded in nonisothermal crystallization of neat PBA (a), PBA in PVDF/PBA blends with PVDF isothermally crystallized at different T_{IC,PVDF}'s, (c,e) and their following heating processes (b, d, and f). Different cooling rates (1–15 °C/min) were used for neat PBA (a), and a fixed cooling rate of 10 °C/min was used for the PBA component in blends (c,e).

DSC curves recorded in the nonisothermal crystallization and subsequent heating processes for the neat PBA with T_f = 200 °C and the PBA component in PVDF/PBA blends (C_{PVDF} = 50 and 75%) with PVDF isothermally crystallized at various T_{IC,PVDF}'s. As seen in Figure 7a and b, the α, β, and α/β mixed crystals are, respectively, produced at the cooling rate of ≤2.5, ≥15, and 5–10 °C/min, consistent with the previous reports.^{7,9} The crystallization and melting behavior of neat PBA with the different T_f's (80–140 °C) and cooling rates were also investigated under the thermal procedure shown in Figure 1c, and a similar cooling rate dependence of the melting behavior was found (data not shown). The nonisothermal crystallization and subsequent melting behavior of neat PBA depend on the cooling rate but not the T_f when T_f is much higher than T_{m,PBA}.

In the case of PVDF/PBA blends, the nonisothermal crystallization of the PBA component depends on T_{IC,PVDF}. Two points should be noted in Figure 7c and e. First, two

separated crystallization peaks (indicated by 1 and 2), that is, fractional crystallization, are found in the cooling process of PBA for the blends with PVDF crystallized at T_{IC,PVDF} = 140 °C. However, only one peak is present for the blend with a lower T_{IC,PVDF} (80–120 °C). Second, as seen in Figure 7d and f, only the melting peaks of PBA α crystals are detected in the blends with PVDF crystallized at a low T_{IC,PVDF} (80–120 °C), but the melting characteristics of both α and β crystals are present at a high T_{IC,PVDF} (140 °C). This coincides with the WAXD results shown in Figure 6. The T_{IC,PVDF} effects on the crystalline structure of PBA in nonisothermal crystallization is attributable to its crystallization temperature. The fractional crystallization decreases the crystallization temperature of partial PBA, and thus, the α/β mixed crystals are formed in the cooling process of the blends with T_{IC,PVDF} = 140 °C. The crystallization temperature of PBA increases with decreasing T_{IC,PVDF} from 140 to 80 °C, and thus, a lower T_{IC,PVDF} facilitates the formation of α-form PBA.

The crystallization enthalpy (ΔH_c) during cooling and the melting enthalpy (ΔH_m) during subsequent heating for the PBA component in the blends with different C_{PVDF}'s are listed in Table 1. In the blends with C_{PVDF} = 90%, no discernible crystallization and melting of PBA is observed because of the dilution effect. As seen in Table 1, both ΔH_c and ΔH_m of PBA decreases with an increase in C_{PVDF}, indicative of the decrease of PBA crystallinity. This can be ascribable to the confinement effects of PVDF on the crystallization of PBA.

3.3. Morphological Analysis by SAXS. To elucidate the T_{IC,PVDF} effects on phase distribution of the PBA component in the blends, neat PVDF, PBA, and PVDF/PBA blends with PVDF crystallized at lower and higher T_{IC,PVDF}'s were analyzed by SAXS. Lorentz-corrected SAXS profiles of neat PVDF, PBA, and their blends with different thermal treatments are shown in Figure 8. In these profiles, the scattering vector is $q = 4\pi \sin \theta / \lambda$

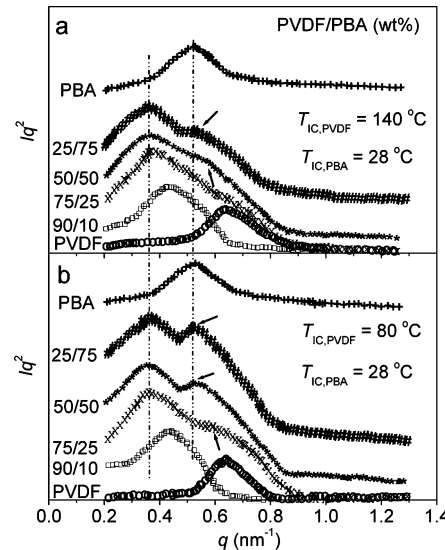


Figure 8. Lorentz-corrected SAXS profiles of neat PVDF, PBA, and their blends with various C_{PVDF}'s after the sequential crystallizations of PVDF at T_{IC,PVDF} = 140 (a) or 80 °C (b) and PBA at T_{IC,PBA} = 28 °C. The profiles were vertically shifted for clarity.

λ , where 2θ and λ are, respectively, the scattering angle and wavelength and Iq² represents the relative intensity.^{34,35} The long period (LP), the sum of the thickness of the crystalline lamellar layer (L_c) and the amorphous layer (L_a), can be

calculated from $LP = 2\pi/q^*$, where q^* corresponds to the peak observed in the Lorentz-corrected SAXS profile.³⁴

As seen in Figure 8a, the q^* value of neat PVDF (0.63 nm^{-1}) is larger than that of neat PBA (0.51 nm^{-1}). At $T_{IC,PVDF} = 140^\circ\text{C}$, the q^* value shifts to the low- q region (0.45 or 0.37 nm^{-1}) after blending with a small amount of PBA ($C_{PBA} = 10$ or $25 \text{ wt } \%$), indicative of the increase in LP of the PVDF component. This can be ascribed to the segregation of PBA to the interlamellar region of PVDF. In the blend with $C_{PBA} = 50 \text{ wt } \%$, a weak shoulder is observed at $q = 0.60 \text{ nm}^{-1}$, except for the predominant peak at 0.37 nm^{-1} . The shoulder peak would be ascribed to the PBA component because a part of PBA may be excluded from the interlamellar region of PVDF and enter into the interspherulitic or interfibrillar region of PVDF with the formation of an individual crystalline phase.³⁴ With a further increase in C_{PBA} ($75 \text{ wt } \%$), LP of the PVDF phase remains unchanged, and the peak related to PBA further shifts to lower q^* (0.55 nm^{-1}), which is almost the same as that of neat PBA (0.53 nm^{-1}). This suggests that more PBA may tend to accumulate in the interspherulitic or interfibrillar region of PVDF with an increase of C_{PBA} .

However, for the blends with $T_{IC,PVDF} = 80^\circ\text{C}$, a distinct shoulder peak is detected at around $q = 0.60 \text{ nm}^{-1}$ in the blends with $C_{PBA} = 25 \text{ wt } \%$ (Figure 8b). By comparing parts a and b of Figure 8, one can clearly see that at the same blend compositions, the shoulder peak at 0.53 – 0.60 nm^{-1} , which is possibly ascribed to the crystalline phase of PBA located in the interspherulitic or interfibrillar region of PVDF, is larger in magnitude for the samples with $T_{IC,PVDF} = 80^\circ\text{C}$ than those with $T_{IC,PVDF} = 140^\circ\text{C}$. It is reasonable to conclude that $T_{IC,PVDF}$ is a key factor affecting the crystalline morphology of PVDF/PBA blends and the lower $T_{IC,PVDF}$ may favor the segregation of PBA in the interspherulitic or interfibrillar region of PVDF.

The fractional crystallization of PBA in the blends with a higher $T_{IC,PVDF}$ can be ascribed to its phase segregation and distribution during the crystallization of PVDF. Peaks 1 and 2 in Figure 7c and e are considered to be attributed to the crystallization of PBA segregated in the interspherulitic/interfibrillar and interlamellar regions of PVDF, respectively. As compared to the interspherulitic/interfibrillar region, the confined interlamellar region would limit the motion and rearrangement of the molecular chains. Thus, PBA segregated into the interlamellar region of the PVDF crystalline phase would be difficult to crystallize and thus needs a large degree of supercooling. The effects of crystallization conditions of PVDF on the fractional crystallization of PBA in blends are consistent with the results of PBS/PEO blends.^{22,23} However, we cannot give an exact explanation to this phenomenon of $T_{IC,PVDF}$ -dependent phase segregation of the PBA component on the basis of the present data. The in-depth mechanistic investigations will be conducted in a future study.

3.4. β -to- α Phase Transition of PBA in Blends upon Annealing.

Effects of the crystallization conditions of PVDF on the β -to- α phase transition of PBA were investigated by WAXD. Figure 9 shows the WAXD patterns of PVDF/PBA blends ($C_{PVDF} = 50\%$) containing the β -form PBA after annealing at 48°C for different periods. The β crystals of PBA in the blends were produced by isothermal crystallization at $T_{IC,PBA} = 18^\circ\text{C}$ after the crystallization of PVDF at $T_{IC,PVDF} = 80$ or 140°C . As seen in Figure 9, after annealing at 48°C , the (110) and (020) peaks of PBA β crystals gradually weaken, and the (110) and (021) peaks of PBA α crystals become more

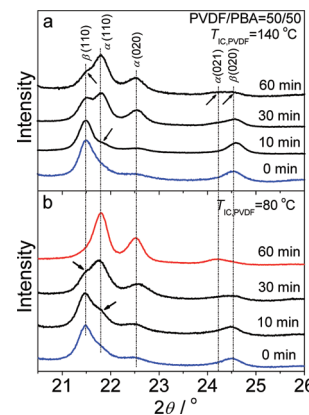


Figure 9. WAXD patterns of PVDF/PBA blends ($C_{PVDF} = 50\%$) after annealing at 48°C for different periods. Before annealing, the samples were treated by the sequential crystallizations of PVDF at $T_{IC,PVDF} = 140^\circ\text{C}$ (a) or 80°C (b) and PBA at $T_{IC,PBA} = 18^\circ\text{C}$ to produce the pure β crystals of PBA.

distinct, indicative of the β -to- α phase transition. Interestingly, the lower $T_{IC,PVDF}$ facilitates the β -to- α phase transition of PBA in the PVDF/PBA blends during annealing at an elevated temperature. All of the β crystals of PBA transform to their α counterparts after annealing at 48°C for 60 min in the blend with $T_{IC,PVDF} = 80^\circ\text{C}$ (Figure 9b). However, partial β crystals still exist in the blends with $T_{IC,PVDF} = 140^\circ\text{C}$ after annealing under the same conditions (Figure 9a). Similar results were also found for the blends with other compositions (data not shown).

To examine the structural change of PBA crystals upon annealing, the ratio of the α phase to the total crystalline phase (including α and β phases) of PBA, denoted as $\alpha\%$, was quantitatively estimated via fitting of the WAXD profiles.²⁹ $\alpha\%$ equals to the area ratio of the diffraction peak of the α phase to that of the whole crystalline phase of PBA. $\alpha\%$ values of the PBA component are shown in Table 2. Under the same

Table 2. Dependences of $\alpha\%$ of PBA on Annealing Time in the Blends with Different C_{PVDF} s and $T_{IC,PVDF}$ s

sample	$T_{IC,PVDF} = 140^\circ\text{C}$			$T_{IC,PVDF} = 80^\circ\text{C}$		
	$t_a = 10$ min	$t_a = 30$ min	$t_a = 60$ min	$t_a = 10$ min	$t_a = 30$ min	$t_a = 60$ min
PVDF/PBA = 10/90	87	100	100	100	100	100
PVDF/PBA = 25/75	54	84	100	70	100	100
PVDF/PBA = 50/50	25	73	88	38	85	100
PVDF/PBA = 75/25	19	62	78	28	76	88
PVDF/PBA = 90/10	UD ^a	UD	UD	UD	UD	UD

^aUnable to determine.

conditions ($T_{IC,PVDF}$ and t_a), an increase in C_{PVDF} leads to a decrease of $\alpha\%$ and the β -to- α transition rate because of the increased confinement effects of PVDF on the rearrangement and motion of PBA molecular chains. At the same t_a and blend composition, $\alpha\%$ is larger in the blends with a lower $T_{IC,PVDF}$ (80°C) than that with a higher $T_{IC,PVDF}$ (140°C), indicating that the lower $T_{IC,PVDF}$ facilitates the β -to- α phase transition of PBA. As mentioned above, $T_{c,\alpha}$ and T_m^0 of the PBA α crystals

in the blends with a lower $T_{IC,PVDF}$ are lower than those with a higher $T_{IC,PVDF}$. Therefore, under the same annealing temperature (T_a), there is bigger temperature gap between T_a and $T_{c,\alpha}$ ($T_a - T_{c,\alpha}$) and a smaller temperature gap between T_a and T_m^0 ($T_m^0 - T_a$) for the blends with a lower $T_{IC,PVDF}$, which would be more energetically favorable for the annealing-induced phase transition. Furthermore, because PBA tends to segregate in the interlamellar region of the PVDF phase at a higher $T_{IC,PVDF}$ (140 °C), the confinement effects of the PVDF crystalline lamellae may impede the rearrangement and reorganization of PBA molecular chains. This could retard the β -to- α transition of PBA upon annealing.

3.5. Enzymatic Degradation. The effects of $T_{IC,PVDF}$ on enzymatic degradation of the PBA component in the PVDF/PBA blends were investigated. Because PVDF cannot be degraded by lipase, the morphology and weight changes of blend samples after degradation are correlated to the PBA phase. Figure 10 shows the weight loss of PBA in the blends

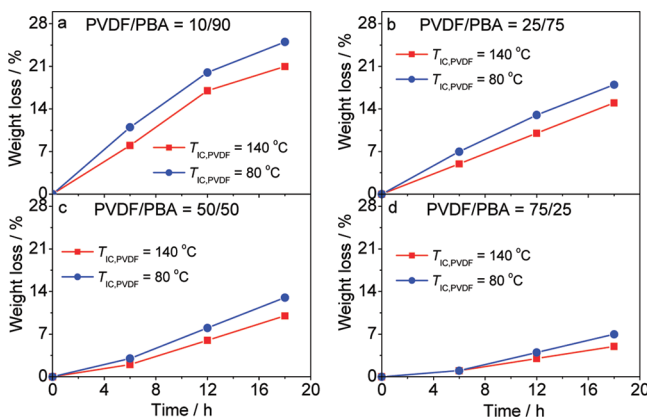
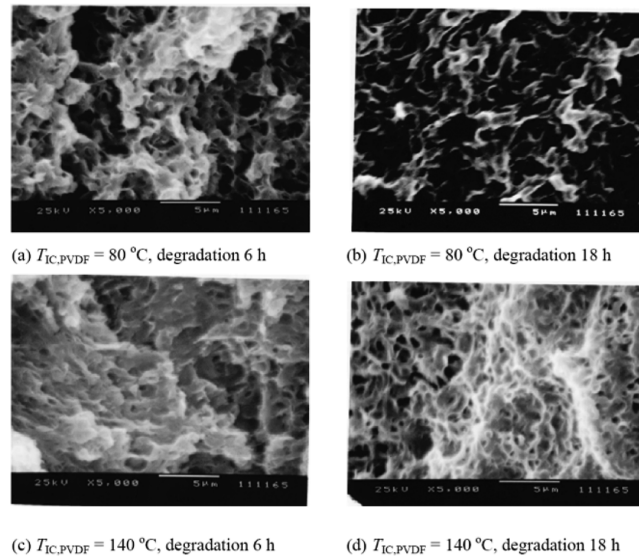


Figure 10. Weight loss of PBA in PVDF/PBA blends with different C_{PVDF} 's after degradation for various periods. Before degradation, the blends were treated by the sequential crystallizations of PVDF at $T_{IC,PVDF} = 80$ or 140 °C and PBA at $T_{IC,PBA} = 28$ °C.

with different compositions. Weight loss was calculated from the ratio of the decreased weight to the initial weight of the PBA component in the blends. As seen in Figure 10, the degradation of the PBA component in the blends with a lower $T_{IC,PVDF}$ is clearly faster than those with a higher $T_{IC,PVDF}$. Figure 11 shows the SEM pictures of the film surface for the blends ($C_{PVDF} = 50\%$) with different $T_{IC,PVDF}$'s and degradation times. Consistent with the results of weight loss, larger and deeper cavities are present in the blends with $T_{IC,PVDF} = 80$ °C than those with $T_{IC,PVDF} = 140$ °C.

Effects of $T_{IC,PVDF}$ on the degradation rate of PBA in the blends can be correlated with its crystalline structure. As indicated in the aforementioned WAXD and FTIR results, the pure α and α/β mixed crystals are formed at $T_{IC,PBA} = 28$ °C in the blends with $T_{IC,PVDF} = 80$ and 140 °C, respectively. Gan et al. have reported that the α crystals degrade faster than the β or α/β mixed crystals.³⁷ Therefore, the enzymatic degradation rate of PBA increases with a decrease in $T_{IC,PVDF}$ in the blends. On the other hand, with increasing the PVDF fraction, the degradation rate of PBA becomes slow (Figure 10), even though there is a decrease of PBA crystallinity (Table 1). This is attributable to the physical confinement effect of PVDF crystals, which prevents the direct contact and attack of lipase to the PBA phase.



(a) $T_{IC,PVDF} = 80$ °C, degradation 6 h (b) $T_{IC,PVDF} = 80$ °C, degradation 18 h
(c) $T_{IC,PVDF} = 140$ °C, degradation 6 h (d) $T_{IC,PVDF} = 140$ °C, degradation 18 h

Figure 11. SEM images of the PVDF/PBA blend ($C_{PVDF} = 50\%$) after enzymatic degradation for 6 (a,c) and 18 h (b,d). Before degradation, the blends were treated by the sequential crystallizations of PVDF at $T_{IC,PVDF} = 80$ (a,b) or 140 °C (c,d) and PBA at $T_{IC,PBA} = 28$ °C.

4. CONCLUSION

Effects of $T_{IC,PVDF}$ on the crystal modification, fractional crystallization, crystalline morphology, and enzymatic degradation of PBA in the PVDF/PBA blends have been studied. Lower $T_{IC,PVDF}$ facilitates the formation of PBA α crystals in both the isothermal and nonisothermal processes and is also favorable for the β -to- α phase transition of PBA upon annealing at an elevated temperature. The fractional crystallization of PBA occurs in the blends with a higher $T_{IC,PVDF}$, possibly attributed to the favorable segregation of PBA in the interlamellar regions of PVDF under these conditions. Because of the effects of the crystalline structure, a decrease in $T_{IC,PVDF}$ results in an increase in the enzymatic degradation rate of PBA. In conclusion, this study elucidates the correlations between $T_{IC,PVDF}$, the crystalline structure, and biodegradation of PBA in the PVDF/PBA blends and furthermore provides a novel approach to manipulate the crystal modification and physical properties of polymorphic polymers in their binary crystalline/crystalline blend systems.

■ AUTHOR INFORMATION

Corresponding Author

*E-mail: jinjun.tit@gmail.com (J.Yang); panpengju@zju.edu.cn (P.P.). Tel./Fax: +86-571-87951334.

■ REFERENCES

- Pan, P.; Inoue, Y. *Prog. Polym. Sci.* **2009**, *34*, 605.
- De Rosa, C.; Auricemma, F. *Prog. Polym. Sci.* **2006**, *31*, 145.
- Brückner, S.; Meille, S. V.; Petraccone, V.; Pirozzi, B. *Prog. Polym. Sci.* **1991**, *16*, 361.
- Lotz, B.; Wittmann, J. C.; Lovinger, A. J. *Polymer* **1996**, *37*, 4979.
- Hoogsteen, W.; Postema, A. R.; Pennings, A. J.; ten Brinke, G. *Macromolecules* **1990**, *23*, 634.
- Furuhashi, Y.; Iwata, T.; Kimura, Y.; Doi, Y. *Macromol. Biosci.* **2003**, *3*, 462.
- Gan, Z.; Abe, H.; Doi, Y. *Macromol. Chem. Phys.* **2002**, *203*, 2369.
- Gan, Z.; Kuwabara, K.; Abe, H.; Iwata, T.; Doi, Y. *Biomacromolecules* **2004**, *5*, 371.

- (9) Woo, E. M.; Wu, M. C. *J. Polym. Sci., Part B: Polym. Phys.* **2005**, *43*, 1662.
- (10) Woo, E. M.; Sun, Y. S.; Yang, C. P. *Prog. Polym. Sci.* **2001**, *26*, 945.
- (11) Wu, M. C.; Woo, E. M. *Polym. Int.* **2005**, *54*, 1681.
- (12) Wittmann, J. C.; Lotz, B. *Prog. Polym. Sci.* **1990**, *15*, 909.
- (13) Cartier, L.; Okihara, T.; Ikada, Y.; Tsuji, H.; Puiggallí, J.; Lotz, B. *Polymer* **2000**, *41*, 8909.
- (14) Sun, Y.; Li, H.; Huang, Y.; Chen, E.; Zhao, L.; Gan, Z.; Yan, S. *Macromolecules* **2005**, *38*, 2739.
- (15) Sun, Y.; Li, H.; Huang, Y.; Chen, E.; Gan, Z.; Yan, S. *Polymer* **2006**, *47*, 2455.
- (16) Libster, D.; Aserin, A.; Garti, N. *Polym. Adv. Technol.* **2007**, *18*, 685.
- (17) Miyazaki, T.; Takeda, Y.; Akasaka, M.; Sakai, M.; Hoshiko, A. *Macromolecules* **2008**, *41*, 2749.
- (18) Jiang, N.; Zhao, L.; Gan, Z. *Polym. Degrad. Stab.* **2010**, *95*, 1045.
- (19) Dong, T.; Kai, W.; Inoue, Y. *Macromolecules* **2007**, *40*, 8285.
- (20) Wang, T.; Li, H.; Wang, F.; Yan, S.; Schultz, J. M. *J. Phys. Chem. B* **2011**, *115*, 7814.
- (21) Wang, T.; Li, H.; Wang, F.; Schultz, J. M.; Yan, S. *Polym. Chem.* **2011**, *2*, 1688.
- (22) He, Y.; Zhu, B.; Kai, W.; Inoue, Y. *Macromolecules* **2004**, *37*, 3337.
- (23) He, Y.; Zhu, B.; Kai, W.; Inoue, Y. *Macromolecules* **2004**, *37*, 8050.
- (24) Wang, H.; Gan, Z.; Schultz, J. M.; Yan, S. *Polymer* **2008**, *49*, 2342.
- (25) Chiu, F. C.; Li, M. T. *Polymer* **2003**, *44*, 8013.
- (26) Wang, C.; Lin, C. C.; Chu, C. P. *Macromolecules* **2006**, *39*, 9267.
- (27) Lee, K. H.; Givens, S. R.; Snively, C. M.; Chase, B.; Rabolt, J. F. *Macromolecules* **2008**, *41*, 3144.
- (28) Pan, P.; Liang, Z.; Zhu, B.; Dong, T.; Inoue, Y. *Macromolecules* **2009**, *42*, 3374.
- (29) Yang, J.; Pan, P.; Hua, L.; Zhu, B.; Dong, T.; Inoue, Y. *Macromolecules* **2010**, *43*, 8610.
- (30) Penning, J. P.; John Manley, R. S. *Macromolecules* **1996**, *29*, 77.
- (31) Penning, J. P.; John Manley, R. S. *Macromolecules* **1996**, *29*, 84.
- (32) Fujita, K.; Kyu, T.; John Manley, R. S. *Macromolecules* **1996**, *29*, 91.
- (33) Isayeva, I.; Kyu, T.; John Manley, R. S. *Polymer* **1998**, *39*, 4599.
- (34) Liu, L.; Chu, B.; Penning, J. P.; John Manley, R. S. *Macromolecules* **1997**, *30*, 4398.
- (35) Liu, L.; Chu, B.; Penning, J. P.; John Manley, R. S. *J. Polym. Sci., Part B: Polym. Phys.* **2000**, *38*, 2296.
- (36) Gan, Z.; Kuwabara, K.; Abe, H.; Iwata, T.; Doi, Y. *Polym. Degrad. Stab.* **2005**, *87*, 191.
- (37) Zhao, L.; Gan, Z. *Polym. Degrad. Stab.* **2006**, *91*, 2429.
- (38) Yang, J.; Li, Z.; Pan, P.; Zhu, B.; Dong, T.; Inoue, Y. *J. Polym. Sci., Part B: Polym. Phys.* **2009**, *47*, 1997.
- (39) Yan, C.; Zhang, Y.; Hu, Y.; Ozaki, Y.; Shen, D.; Gan, Z.; Yan, S.; Takahashi, I. *J. Phys. Chem. B* **2008**, *112*, 3311.
- (40) Hoffman, J. D.; Weeks, J. J. *J. Res. Natl. Bur. Stand.* **1962**, *66A*, 13.